ELSEVIER

J. Non-Newtonian Fluid Mech. 111 (2003) 87–105

Journal of Non-Newtonian Fluid Mechanics

www.elsevier.com/locate/jnnfm

Viscoelastic potential flow analysis of capillary instability

T. Funada [a], D.D. Joseph [b,*]

[a] *Department of Digital Engineering, Numazu College of Technology, Ooka 3600, Numazu, Shizuoka, Japan*

[b] *Department of Aerospace Engineering and Mechanics, University of Minnesota, 110 Union St. SE, Minneapolis, MN 55455, USA*

Received 24 July 2002; received in revised form 7 December 2002

Abstract

Analysis of the linear theory of capillary instability of threads of Maxwell fluids of diameter D is carried out for the unapproximated normal mode solution and for a solution based on viscoelastic potential flow. The analysis here extends the analysis of viscous potential flow [Int. J. Multiphase Flow 28 (2002) 1459] to viscoelastic fluids of Maxwell type. The analysis is framed in dimensionless variables with a velocity scale based on the natural collapse velocity $V = \gamma/\mu$ (surface tension/liquid viscosity). The collapse is controlled by two dimensionless parameters, a Reynolds number $J = VD\rho/\mu = \rho\gamma D/\mu^2 = (Oh)^2$ where Oh is the Ohnesorge number, and a Deborah number $\Lambda_1 = \lambda_1 V/D$ where λ_1 is the relaxation time. The density ratio ρ_a/ρ and μ_a/μ are nearly zero and do not have a significant effect on growth rates. The dispersion relation for viscoelastic potential flow is cubic in the growth rate σ and it can be solved explicitly and computed without restrictions on the Deborah number. On the other hand, the iterative procedure used to solve the dispersion relation for fully viscoelastic flow fails to converge at very high Deborah number. The growth rates in both theories increase with Deborah number at each fixed Reynolds number, and all theories collapse to inviscid potential flow (IPF) for any fixed Deborah number as the Reynolds number tends to infinity.

Keywords: Instability; Capillary; Viscoelastic; Viscous; Inviscid; Oldroyd

1. Introduction

Capillary instability of a liquid cylinder of mean radius R leading to capillary collapse can be described as a neckdown due to surface tension γ in which fluid is ejected from the throat of the neck, leading to a smaller neck and greater neckdown capillary force as seen in Fig. 1.

* Corresponding author. Tel.: +1-612-625-0309; fax: +1-612-626-1558.
E-mail address: joseph@aem.umn.edu (D.D. Joseph).

0377-0257/03/$ – see front matter © 2003 Elsevier Science B.V. All rights reserved.
doi:10.1016/S0377-0257(03)00013-2

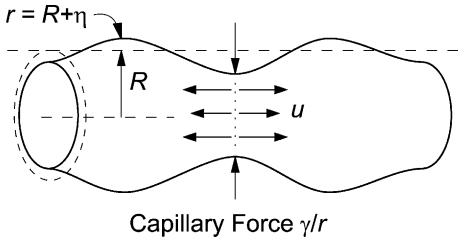

Fig. 1. Capillary instability. The force γ/r forces fluid from the throat, decreasing r leading to collapse.

The dynamical theory of instability of a long cylindrical column of liquid of radius R under the action of capillary force was given by Rayleigh [1] following earlier work by Plateau [2] who showed that a long cylinder of liquid is unstable to disturbances with wavelengths greater than $2\pi R$. Rayleigh showed that the effect of inertia is such that the wavelength λ corresponding to the mode of maximum instability is $\lambda = 4.51 \times 2R$, exceeding very considerably the circumference of the cylinder. The idea that the wave length associated with fastest growing growth rate would become dominant and be observed in practice was first put forward by Rayleigh [1]. The analysis of Rayleigh is based on potential flow of an inviscid liquid neglecting the effect of the outside fluid. (Looking forward, we here note that it is possible and useful to do an analysis of this problem based on the potential flow of a viscoelastic fluid.)

An attempt to account for viscous effects was made by Rayleigh [3] again neglecting the effect of the surrounding fluid. One of the effects considered is meant to account for the forward motion of an inviscid fluid with a resistance proportional to velocity. The effect of viscosity is treated in the special case in which the viscosity is so great that inertia may be neglected. He shows that the wavelength for maximum growth is very large, strictly infinite. He says, "... long threads do not tend to divide themselves into drops at mutual distances comparable to with the diameter of the cylinder, but rather to give way by attenuation at few and distant places."

Weber [4] extended Rayleigh's theory by considering an effect of viscosity and that of surrounding air on the stability of a columnar jet. He showed that viscosity does not alter the value of the cut-off wavenumber predicted by the inviscid theory and that the influence of the ambient air is not significant if the forward speed of the jet is small. Indeed the effects of the ambient fluid, which can be liquid or gas, might be significant in various circumstances. The problem, yet to be considered for liquid jets, is the superposition of Kelvin–Helmholtz and capillary instability.

Tomotika [5] considered the stability to axisymmetric disturbances of a long cylindrical column of viscous liquid in another viscous fluid under the supposition that the fluids are not driven to move relative to one another. He derived the dispersion relation for the fully viscous case (his(33)); he solved it only under the assumption that the time derivative in the equation of motion can be neglected but the time derivative in the kinematic condition is taken into account (his(34)). These approximations lead herein to the asymptotic solution in the limit of $J \to 0$.

The effect of viscosity on the stability of a liquid cylinder when the surrounding fluid is neglected and on a hollow (dynamically passive) cylinder in a viscous liquid was treated briefly by Chandrasekhar [6]. The parameter $\gamma R\rho/\mu^2$ which can be identified as a Reynolds number based on a velocity γ/μ and the viscosity of the liquid μ, appears in the dispersion relation derived there.

Eggers [7] has given a comprehensive review of nonlinear dynamics and breakup of free surface flows of Newtonian fluids. All of the references just mentioned are discussed in the Eggers review.

Tomotika's problem was studied by Lee and Flumerfelt [8] without making the approximations used by Tomotika, focusing on the elucidation of various limiting cases defined in terms of three dimensionless parameter, a density ratio, a viscosity ratio and the Ohnesorge number $Oh = \sqrt{\rho\gamma D}/\mu = J^{1/2}$.

It is perhaps necessary to call attention to the fact it is neither necessary nor desirable to put the viscosities to zero when considering potential flows. The Navier–Stokes equations, and the equations for many models of a viscoelastic fluid, are satisfied by potential flow; the viscous term is identically zero when the vorticity is zero but the viscous stresses are not zero [9]. It is not possible to satisfy the no-slip condition at a solid boundary or the continuity of the tangential component of velocity and shear stress at a fluid–fluid boundary when the velocity is given by a potential. The viscous stresses enter into the viscous potential flow analysis of free surface problems through the normal stress balance at the interface. Viscous potential flow analysis gives good approximations to fully viscous flows in cases where the shears from the gas flow are negligible; the Rayleigh–Plesset bubble is a potential flow which satisfies the Navier–Stokes equations and all the interface conditions. Joseph et al. [10] constructed a viscous potential flow analysis of the Rayleigh–Taylor instability which can scarcely be distinguished from the exact fully viscous analysis. Similar agreements were demonstrated for viscoelastic fluids by Joseph et al. [11]. In a recent paper, Funada and Joseph [12] analyzed Kelvin–Helmholtz instability of a plane gas–liquid layer using viscous potential flow.

Funada and Joseph [13] did a viscous potential flow analysis of capillary instability. Results of linearized analysis based on potential flow of a viscous and inviscid fluid are compared with the unapproximated normal mode analysis of the linearized Navier–Stokes equations. The growth rates for the inviscid fluid are largest, the growth rates of the fully viscous problem are smallest and those of viscous potential flow are between. They found that the results from all three theories converge when J is large with reasonable agreement between viscous potential and fully viscous flow with $J > \mathrm{O}(10)$. The convergence results apply to two liquids as well as to liquid and gas.

In this paper, we shall extend the results of Funada and Joseph [13] to the case of viscoelastic liquid filaments of Maxwell type. Joseph et al. [11] have analyzed Rayleigh–Taylor instability of an Oldroyd fluid using viscoelastic potential flow. They show that the most unstable wave is a sensitive function of the retardation time λ_2 which fits experiments when $\lambda_2/\lambda_1 = \mathrm{O}(10^{-3})$. The growth rates for the most unstable wave are much larger than for the comparable viscous drop, which agrees with the surprising fact that the breakup times for viscoelastic drops are shorter. They also do an analysis of Rayleigh–Taylor instability based on viscoelastic potential flow which gives rise to nearly the same dispersion relation as the unapproximated analysis.

The linear stability analysis of the capillary instability of a viscoelastic fluid has been done by Middleman [14] and Goldin et al. [15]. They showed that the growth rates are larger for the viscoelastic fluid. The analysis done here of viscoelastic potential flow has not been done before.

Chang et al. [16] did a long wave study of the stretching dynamics of bead-string filaments for FENE and Oldroyd-B fluids which extends the results of Bousfield et al. [17]. They also do a long wave study of linear stability of the cylinder studied here in the small J limit. Strictly speaking, the long wave equations perturb solutions with infinitely long wavelengths. The wavelength for the maximum growth rates computed here range from $20\pi D$ to a little less than $2\pi D$.

Bousfield et al. [17] did a nonlinear analysis of capillary instability which captures observed features of the breakup in experiments cited by them better than the linear theory.

A referee of this paper noted that the observed increase of stability of jets with increasing elasticity, which contradicts the results of the linear stability analysis given here and elsewhere, may possibly be

explained by linear stability analysis of a stressed filament at rest (see [18] for a simplified analysis). One difficulty is that a stressed filament at rest is not a permanent solution.

The analysis which is developed in the sections to follow is framed in a general way suitable for an Oldroyd-B filament in another viscous fluid which is designated with a subscript 'a', for air. The linear theory perturbs a uniform cylinder with capillary forces. It is well known that all small perturbations of motionless states are governed by the constitutive equation of linear viscoelastic fluids ([19], section 164):

$$\left[1+\lambda_1\frac{\partial}{\partial t}\right]\tau=\mu_0\left[1+\lambda_2\frac{\partial}{\partial t}\right]\left[\nabla\vec{v}+(\nabla\vec{v})^{\mathrm{T}}\right], \tag{1}$$

where τ is the viscous stress tensor, μ_0 the viscosity, and $1/2[\nabla\vec{v}+(\nabla\vec{v})^{\mathrm{T}}]$ the rate of strain tensor. Here we have assumed an Oldroyd model so that the parameters of the general linear viscoelastic fluid are expressed in terms of the model parameters.

2. Linear stability for small disturbances of fully viscoelastic flow

In an undisturbed rest state, the long column of liquid (viscoelastic liquid of density ρ and viscosity μ) with mean radius R is put in $0\le r<R$ and the fluid 'a' (air or gas of density ρ_{a} and viscosity μ_{a}) is in $R<r<\infty$, using cylindrical coordinates (r,θ,z). The normal stress balance is given by

$$\bar{p}-\bar{p}_{\mathrm{a}}=\frac{\gamma}{R}, \tag{2}$$

where $\bar{p}$ is the liquid pressure, $\bar{p}_{\mathrm{a}}$ is the gas pressure, and γ denotes the interfacial tension. The stability problem of this state to small axisymmetric disturbances is solved herein.

In terms of the diameter of column D, typical time T, typical velocity $U=D/T$ and typical pressure $p_0=\gamma/D=\rho U^2$ for which $U=\sqrt{\gamma/(\rho D)}$, we have the normalization:

$$\left.\begin{aligned} &r=D\tilde{r}, && z=D\tilde{z}, && t=T\tilde{t},\\ &p=p_0\tilde{p}, && \psi=UD^2\tilde{\psi}, && u=U\tilde{u}, && w=U\tilde{w}, && \eta=D\tilde{\eta}, \end{aligned}\right\} \tag{3}$$

where ψ is the stream function for axisymmetric flow:

$$u=\frac{1}{r}\frac{\partial\psi}{\partial z},\qquad w=-\frac{1}{r}\frac{\partial\psi}{\partial r}. \tag{4}$$

The parameters are given by

$$\left.\begin{aligned} &\ell=\frac{\rho_{\mathrm{a}}}{\rho}, && m=\frac{\mu_{\mathrm{a}}}{\mu_0}, && J=\frac{VD\rho}{\mu_0}=\frac{\rho\gamma D}{\mu_0^2},\\ &\Lambda_1=\frac{\lambda_1 V}{D}, && \hat{\lambda}_1=\frac{\Lambda_1}{\sqrt{J}}, && \Lambda_2=\frac{\lambda_2 V}{D}, && \hat{\lambda}_2=\frac{\Lambda_2}{\sqrt{J}}, \end{aligned}\right\} \tag{5}$$

where $V=\gamma/\mu_0$ denotes the capillary collapse velocity, and Λ_1 is the Deborah number. It is noted that T may also be defined as $T=D/V$ which is suitable for small J, but $T=D/U=(D/V)\sqrt{J}$ is suitable for large J. Hereinafter, dimensionless quantities are used without a tilde.

For small disturbances, the equations for the liquid are given by

$$\frac{\partial u}{\partial r}+\frac{u}{r}+\frac{\partial w}{\partial z}=0, \tag{6}$$

$$\rho\frac{\partial u}{\partial t}=-\frac{\partial p}{\partial r}+\frac{\hat{\mu}}{\sqrt{J}}\left(\nabla^2 u-\frac{u}{r^2}\right), \qquad \rho\frac{\partial w}{\partial t}=-\frac{\partial p}{\partial z}+\frac{\hat{\mu}}{\sqrt{J}}\nabla^2 w, \tag{7}$$

where the constitutive equation is expressed symbolically as

$$\hat{\mu}=\frac{1+\hat{\lambda}_2(\partial/\partial t)}{1+\hat{\lambda}_1(\partial/\partial t)}, \tag{8}$$

and the equations for fluid 'a' are given by

$$\frac{\partial u_{\mathrm{a}}}{\partial r}+\frac{u_{\mathrm{a}}}{r}+\frac{\partial w_{\mathrm{a}}}{\partial z}=0, \tag{9}$$

$$\ell\frac{\partial u_{\mathrm{a}}}{\partial t}=-\frac{\partial p_{\mathrm{a}}}{\partial r}+\frac{m}{\sqrt{J}}\left(\nabla^2 u_{\mathrm{a}}-\frac{u_{\mathrm{a}}}{r^2}\right), \qquad \ell\frac{\partial w_{\mathrm{a}}}{\partial t}=-\frac{\partial p_{\mathrm{a}}}{\partial z}+\frac{m}{\sqrt{J}}\nabla^2 w_{\mathrm{a}}, \tag{10}$$

with the Laplacian defined as

$$\nabla^2=\frac{\partial^2}{\partial r^2}+\frac{1}{r}\frac{\partial}{\partial r}+\frac{\partial^2}{\partial z^2}. \tag{11}$$

The kinematic condition at the interface $r=R+\eta\approx R$ ($R=1/2$) is given for each fluid by

$$\frac{\partial \eta}{\partial t}=u, \qquad \frac{\partial \eta}{\partial t}=u_{\mathrm{a}}, \tag{12}$$

and the normal stress balance at $r\approx R$ is given by

$$p-p_{\mathrm{a}}-2\frac{\hat{\mu}}{\sqrt{J}}\frac{\partial u}{\partial r}+2\frac{m}{\sqrt{J}}\frac{\partial u_{\mathrm{a}}}{\partial r}=-\left(\frac{\partial^2\eta}{\partial z^2}+\frac{\eta}{R^2}\right). \tag{13}$$

The velocity components are continuous across the interface, for which

$$u=u_{\mathrm{a}}, \qquad w=w_{\mathrm{a}}. \tag{14}$$

The tangential stress balance at the interface is given by

$$\frac{\hat{\mu}}{\sqrt{J}}\left(\frac{\partial u}{\partial z}+\frac{\partial w}{\partial r}\right)=\frac{m}{\sqrt{J}}\left(\frac{\partial u_{\mathrm{a}}}{\partial z}+\frac{\partial w_{\mathrm{a}}}{\partial r}\right). \tag{15}$$

The stability problem for the disturbances is given by the Eqs. (6)–(10) and the boundary conditions Eqs. (12)–(15).

The equation of motion gives the pressure p and the equation of vorticity is expressed in terms of ψ:

$$\frac{\partial p}{\partial z}=\left(\mu\nabla^2-\rho\frac{\partial}{\partial t}\right)w, \qquad \left(\mathrm{D}-\frac{\rho}{\mu}\frac{\partial}{\partial t}\right)\mathrm{D}\psi=0, \tag{16}$$

with the operator D defined as

$$\mathrm{D}\psi=\frac{\partial^2\psi}{\partial r^2}-\frac{1}{r}\frac{\partial\psi}{\partial r}+\frac{\partial^2\psi}{\partial z^2}. \tag{17}$$

The solutions for small disturbances may take the following form:

$$\psi = [A_1 r I_1(kr) + A_2 r I_1(k_\mathrm{v} r)] \exp(\sigma t + \iota k z) + \text{c.c.}, \tag{18}$$

$$\psi_\mathrm{a} = [B_1 r K_1(kr) + B_2 r K_1(k_\mathrm{a} r)] \exp(\sigma t + \iota k z) + \text{c.c.}, \tag{19}$$

$$\eta = H \exp(\sigma t + \iota k z) + \text{c.c.}, \tag{20}$$

where the modified Bessel functions of the first order are denoted by I_1 for the first kind and K_1 for the second kind, σ is the complex growth rate and k is the wavenumber. Substitution of (18)–(20) into (12)–(15) leads to the solvability condition, which is given as the dispersion relation of σ:

$$\begin{vmatrix} I_1(kR) & I_1(k_\mathrm{v}R) & K_1(kR) & K_1(k_\mathrm{a}R) \\ kI_0(kR) & k_\mathrm{v} I_0(k_\mathrm{v}R) & -kK_0(kR) & -k_\mathrm{a} K_0(k_\mathrm{a}R) \\ 2\hat{\mu}k^2 I_1(kR) & \hat{\mu}(k^2+k_\mathrm{v}^2) I_1(k_\mathrm{v}R) & 2mk^2 K_1(kR) & m(k^2+k_\mathrm{a}^2) K_1(k_\mathrm{a}R) \\ F_1 & F_2 & F_3 & F_4 \end{vmatrix} = 0, \tag{21}$$

where F_1–F_4 are defined as

$$F_1 = \iota\sigma I_0(kR) + 2\iota \frac{\hat{\mu}k^2}{\sqrt{J}} I_1'(kR) - \left(\frac{1}{R^2} - k^2\right) \iota \frac{k}{\sigma} I_1(kR), \tag{22}$$

$$F_2 = 2\iota \frac{\hat{\mu}kk_\mathrm{v}}{\sqrt{J}} I_1'(k_\mathrm{v}R) - \left(\frac{1}{R^2} - k^2\right) \iota \frac{k}{\sigma} I_1(k_\mathrm{v}R), \tag{23}$$

$$F_3 = -\iota\sigma\ell K_0(kR) + 2\iota \frac{mk^2}{\sqrt{J}} K_1'(kR), \tag{24}$$

$$F_4 = 2\iota \frac{mkk_\mathrm{a}}{\sqrt{J}} K_1'(k_\mathrm{a}R), \tag{25}$$

with k_v and k_a given by

$$k_\mathrm{v} = \sqrt{k^2 + \frac{\sqrt{J}}{\hat{\mu}}\sigma}, \qquad k_\mathrm{a} = \sqrt{k^2 + \frac{\ell\sqrt{J}}{m}\sigma}, \tag{26}$$

and the prime denotes the derivative: $I_1'(kR) = \mathrm{d}I_1(kR)/\mathrm{d}(kR)$. We note again that $\hat{\mu} = (1+\hat{\lambda}_2\sigma)/(1+\hat{\lambda}_1\sigma)$. It is noted that (21) with $\hat{\mu} = 1$ (for $\hat{\lambda}_1 = \hat{\lambda}_2$ or even for steady case $\sigma = 0$) corresponds to (normalized) Eq. (33) in the paper of Tomotika [5], while (21) reduces to (normalized) (34) if (21) is manipulated by assuming both $\sqrt{J}/\hat{\mu}$ and $\ell\sqrt{J}/m$ are small. Comparing with a Newtonian fluid of same viscosity ($\hat{\mu} = 1$), we find readily that $\hat{\mu} = (1+\hat{\lambda}_2\sigma)/(1+\hat{\lambda}_1\sigma) < 1$ if $0 \le \hat{\lambda}_2 < \hat{\lambda}_1$ and $\sigma > 0$, but $\hat{\mu} > 1$ if $0 \le \hat{\lambda}_2 < \hat{\lambda}_1$ and $\sigma < 0$ within $(1+\hat{\lambda}_1\sigma) > 0$. It may be regarded that the viscoelastic fluid of $\hat{\mu} < 1$ has "viscosity" less than the Newtonian. Even for the Oldroyd model, instability arises in $0 < kR < 1$; the critical wavenumber is given by $k_\mathrm{c} = R^{-1} = 2$. Then we have $\sigma = 0$ at the critical and at $k = 0$. Therefore, the fluid in consideration behaves as a Newtonian fluid of same viscosity near the stability boundaries, while as a fluid of less "viscosity" inside those, which we concern here of the onset of instability.

Table 1
Viscoelastic fluid properties and the parameters (after [10])

	2% PAA	2% PO
ρ (g cm^{-3})	0.99	0.99
μ_0 (P)	96.0	350.0
ρ_a (g cm^{-3})	1.947×10^{-3}	1.776×10^{-3}
μ_a (P)	1.8×10^{-4}	1.8×10^{-4}
γ (dyn cm^{-1})	45.0	63.0
λ_1 (s)	0.039	0.21
λ_2 (s)	0.0	0.0
V (cm s^{-1})	0.4688	0.18
U (cm s^{-1}) $(T = D/U)$	6.742	7.977
J	4.834×10^{-3}	5.091×10^{-4}
$\sqrt{J}$	0.06953	0.02256
ℓ	1.967×10^{-3}	1.794×10^{-3}
m	1.875×10^{-6}	5.143×10^{-7}
Λ_1	0.01828	0.0378
Λ_2	0.0	0.0

For the single column given by $\ell = 0$ and $m = 0$, (21) reduces to

$$\begin{vmatrix} 2\hat{\mu}k^2 I_1(kR) & \hat{\mu}\left(k^2 + k_v^2\right) I_1(k_v R) \\ F_1 & F_2 \end{vmatrix} = 0, \tag{27}$$

which involves J, Λ_1 and Λ_2. This may approximate (21) well for viscoelastic fluids with small values of ℓ and m as shown in Table 1. Eq. (27), as well as (21), is to be solved numerically by an implicit iteration method.

For the viscoelastic potential flow, (21) reduces to

$$\begin{vmatrix} I_1(kR) & K_1(kR) \\ F_1 & F_3 \end{vmatrix} = 0, \tag{28}$$

which is arranged as

$$\sigma(\alpha + \ell\alpha_a) + 2\frac{k^2}{\sqrt{J}}(\hat{\mu}\beta + m\beta_a) - \left(\frac{1}{R^2} - k^2\right)\frac{k}{\sigma} = 0, \tag{29}$$

with

$$\alpha = \frac{I_0(kR)}{I_1(kR)}, \qquad \alpha_a = \frac{K_0(kR)}{K_1(kR)}, \qquad \beta = \frac{I_1'(kR)}{I_1(kR)}, \qquad \beta_a = -\frac{K_1'(kR)}{K_1(kR)}. \tag{30}$$

Arranging then (29) using $\hat{\mu} = (1 + \hat{\lambda}_2\sigma)/(1 + \hat{\lambda}_1\sigma)$, we have the cubic equation of σ (the dispersion relation of the viscoelastic potential flow):

$$A\sigma^2(1 + \hat{\lambda}_1\sigma) + 2\frac{k^2}{\sqrt{J}}(B + B_1\sigma)\sigma + C(1 + \hat{\lambda}_1\sigma) = 0, \tag{31}$$

with

$$A = (\alpha + \ell\alpha_{\rm a}), \qquad B = \beta + m\beta_{\rm a}, \qquad B_1 = \hat{\lambda}_2\beta + m\hat{\lambda}_1\beta_{\rm a}, \qquad C = -\left(\frac{1}{R^2} - k^2\right)k, \tag{32}$$

it is easy to have explicit expressions of the solutions of (31).

When $\hat{\mu} = 1$ for which $\hat{\lambda}_1 = \hat{\lambda}_2$, (31) reduces to the quadratic equation (the dispersion relation of the viscous potential flow) to give the solutions σ:

$$\sigma = -\frac{k^2(\beta + m\beta_{\rm a})}{\sqrt{J}(\alpha + \ell\alpha_{\rm a})} \pm \sqrt{\left[\frac{k^2(\beta + m\beta_{\rm a})}{\sqrt{J}(\alpha + \ell\alpha_{\rm a})}\right]^2 + \left(\frac{1}{R^2} - k^2\right)\frac{k}{(\alpha + \ell\alpha_{\rm a})}}. \tag{33}$$

When the viscosity is dominant, σ for instability (with the upper sign in (33)) may be expressed as

$$\sigma = \frac{1}{2}\left(\frac{1}{R^2} - k^2\right)\frac{\sqrt{J}}{k(\beta + m\beta_{\rm a})}, \tag{34}$$

whereas when the viscosity is negligible, σ may be expressed as

$$\sigma = \sqrt{\left(\frac{1}{R^2} - k^2\right)\frac{k}{(\alpha + \ell\alpha_{\rm a})}}. \tag{35}$$

The viscous potential flow analysis includes the inviscid potential flow (IPF) [13].

3. Asymptotic forms in large J, inviscid potential flow

Taking the limit $J \to \infty$ in the system of equations (6)–(15), we have the equations for inviscid fluids, which allows, of course, solutions for inviscid potential flow:

$$\sigma = \pm\sqrt{\left(\frac{1}{R^2} - k^2\right)\frac{k}{\alpha + \ell\alpha_{\rm a}}}. \tag{36}$$

For the single column given by $\ell = 0$, (36) has the following asymptotic form:

$$\sigma = \pm\sqrt{\left(\frac{1}{R^2} - k^2\right)\frac{k}{\alpha}} \approx \pm\sqrt{\frac{k^2}{2R}} = \pm k. \tag{37}$$

Another limiting case needs to be added as inviscid potential flow. If $\hat{\lambda}_1$ is huge but $\hat{\lambda}_2$ is kept fixed, $\hat{\mu}$ goes to zero. In addition, if $m/\sqrt{J}$ is sufficiently small, (29) reduces to give the solutions (36).

4. Asymptotic forms in small J

Assuming $\sigma\sqrt{J}$ is sufficiently small, manipulating the columns in (21) as was made by Tomotika [5], we have the dispersion relation for small $\sigma\sqrt{J}$:

$$\begin{vmatrix} I_1(kR) & kRI_1'(kR) & K_1(kR) & kRK_1'(kR) \\ I_0(kR) & I_0(kR) + kRI_1(kR) & -K_0(kR) & -K_0(kR) + kRK_1(kR) \\ \hat{\mu}I_1(kR) & \hat{\mu}kRI_0(kR) & mK_1(kR) & -mkRK_0(kR) \\ G_1 & G_2 & G_3 & G_4 \end{vmatrix} = 0, \tag{38}$$

Table 2
Peak values

	k_m	σ_m
PAA		
(1) VPF	3.4308758E−01	6.5569461E−02
(2) VPF (Newtonian)	3.4154810E−01	6.4537511E−02
(3) FVF	2.1395718E−01	2.2780113E−02
(4) FVF (Newtonian)	2.1299713E−01	2.2647558E−02
(5) IPF	1.3956612E+00	9.7090853E−01
PO		
(1) VPF	2.0271663E−01	2.2830346E−02
(2) VPF (Newtonian)	1.9910257E−01	2.2009961E−02
(3) FVF	1.2360773E−01	7.5584962E−03
(4) FVF (Newtonian)	1.2250093E−01	7.4646936E−03
(5) IPF	1.3956612E+00	9.7092587E−01

VPF: viscoelastic potential flow, FVF: fully viscoelastic flow, and IPF: inviscid potential flow. 'Newtonian' means the case for which $\Lambda_1 = 0$.

where G_1–G_4 are defined as

$$G_1 = \hat{\mu} I_1'(kR) - (1 - (kR)^2)\frac{\sqrt{J}}{2\sigma R}\frac{I_1(kR)}{kR}, \tag{39}$$

$$G_2 = \hat{\mu}[I_1'(kR) + kRI_1''(kR) - I_0(kR)] - (1 - (kR)^2)\frac{\sqrt{J}}{2\sigma R} I_1'(kR), \tag{40}$$

$$G_3 = mK_1'(kR), \tag{41}$$

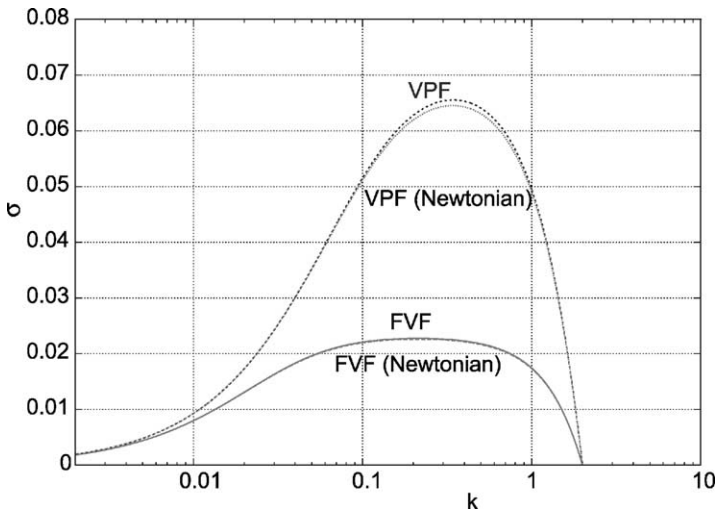

Fig. 2. The growth rate σ vs. k in viscoelastic potential flow (VPF) and fully viscoelastic flow (FVF). PAA as Newtonian and viscoelastic.

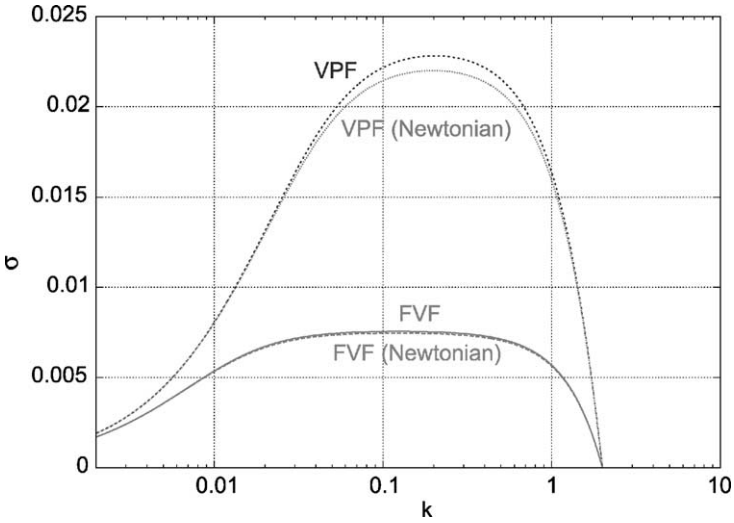

Fig. 3. The growth rate σ vs. k in viscoelasic potential flow (VPF) and fully viscoelasic flow (FVF). PO as Newtonian and viscoelastic.

$$G_4 = m[K_1'(kR) + kRK_1''(kR) + K_0(kR)]. \tag{42}$$

In this limit $J \to 0$, the inertia terms can be neglected, by which ℓ is not included in (38)–(42). We may recall that when $\hat{\mu} = 1$ (viscous fluid), (38) reduces to Tomotika's (normalized) (34) which takes the solution of the form $\sigma =$ (a function of k and m)$\times\sqrt{J}$. Now that $\hat{\mu} = (1 + \hat{\lambda}_2\sigma)/(1 + \hat{\lambda}_1\sigma)$, (38) is the quadratic equation of σ, whose expression is long, thus is omitted here.

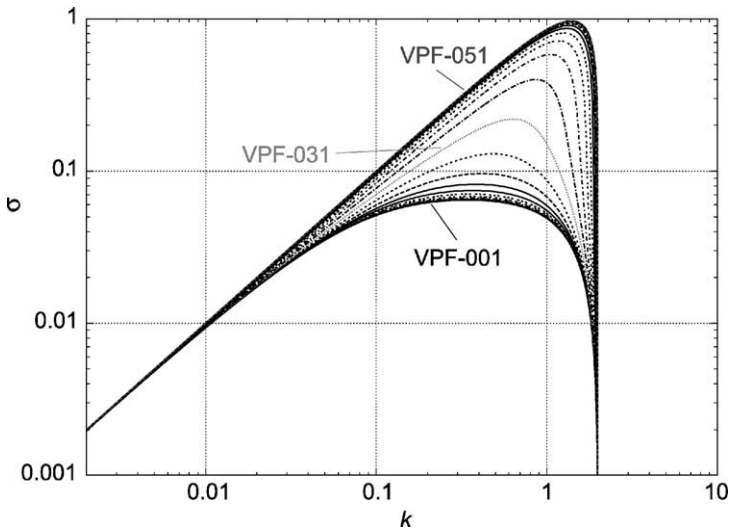

Fig. 4. PAA: VPF $\Lambda_1 = 10^{-6}$ to 10^4. Λ_1 is given as $\Lambda_1 = 10^{(n-31)/5}$ for $n = 1, 2, \ldots, 51$, and n is used to label the curves.

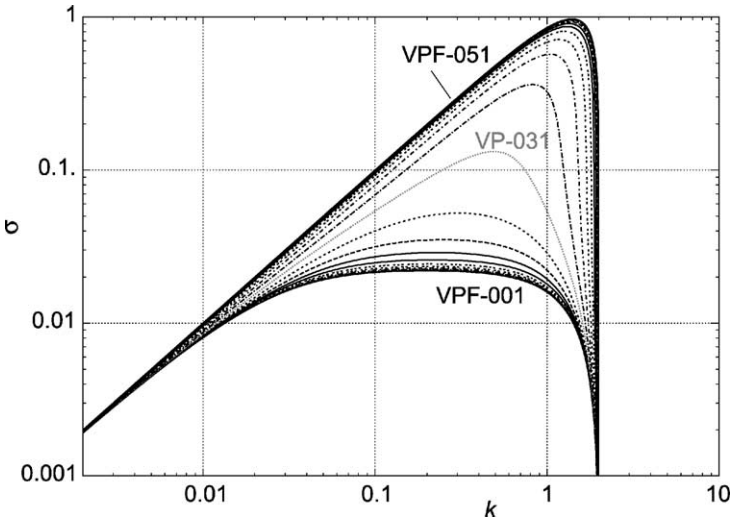

Fig. 5. PO: VPF $\Lambda_1 = 10^{-6}$ to 10^4. Λ_1 is given as $\Lambda_1 = 10^{(n-31)/5}$ for $n = 1, 2, \ldots, 51$, and n is used to label the curves.

For the single column given by $m = 0$, (38) reduces to

$$\begin{vmatrix} \hat{\mu} I_1(kR) & \hat{\mu} kR I_0(kR) \\ G_1 & G_2 \end{vmatrix} = 0, \tag{43}$$

which is arranged as the quadratic equation of σ:

$$\sigma\hat{\mu} = -\frac{\sqrt{J}}{2R} \frac{1 - (kR)^2}{(kR)^2 + 1 - (kR)^2\alpha^2} \equiv f(k). \tag{44}$$

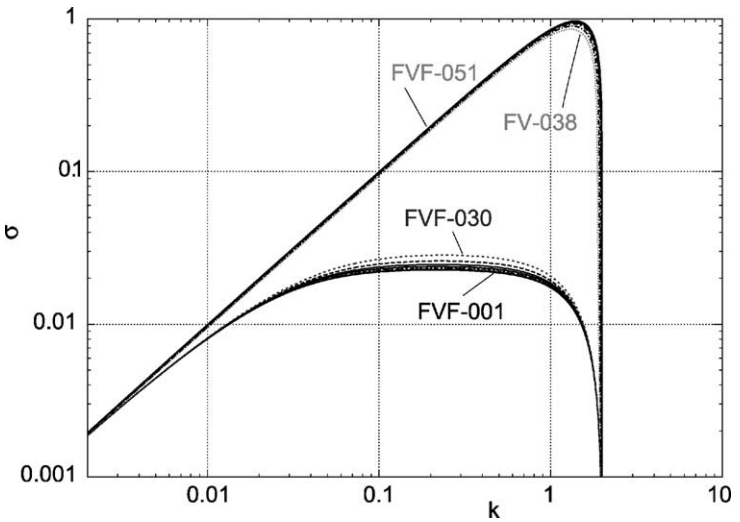

Fig. 6. PAA: FVF $\Lambda_1 = 10^{-6}$ to 10^4. Λ_1 is given as $\Lambda_1 = 10^{(n-31)/5}$ for $n = 1, 2, \ldots, 51$, and n is used to label the curves (curves no. 31–37 are not shown).

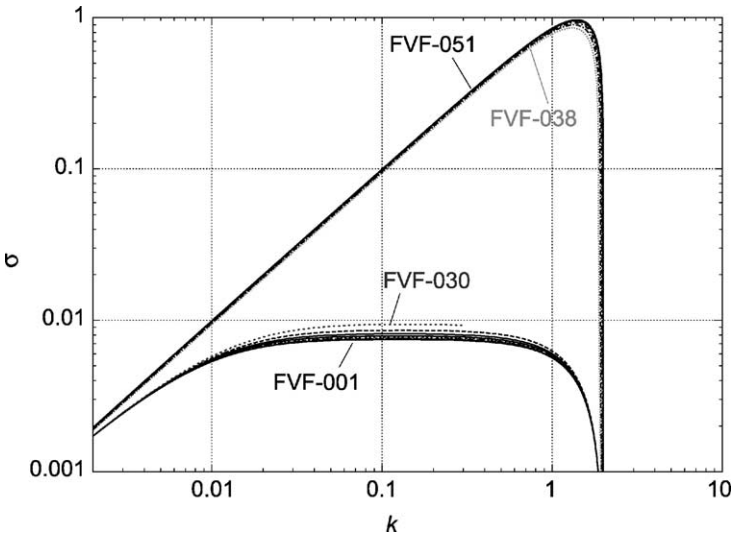

Fig. 7. PO: FVF $\Lambda_1 = 10^{-6}$ to 10^4. Λ_1 is given as $\Lambda_1 = 10^{(n-31)/5}$ for $n = 1, 2, \ldots, 51$, and n is used to label the curves (curves no. 31–37 are not shown).

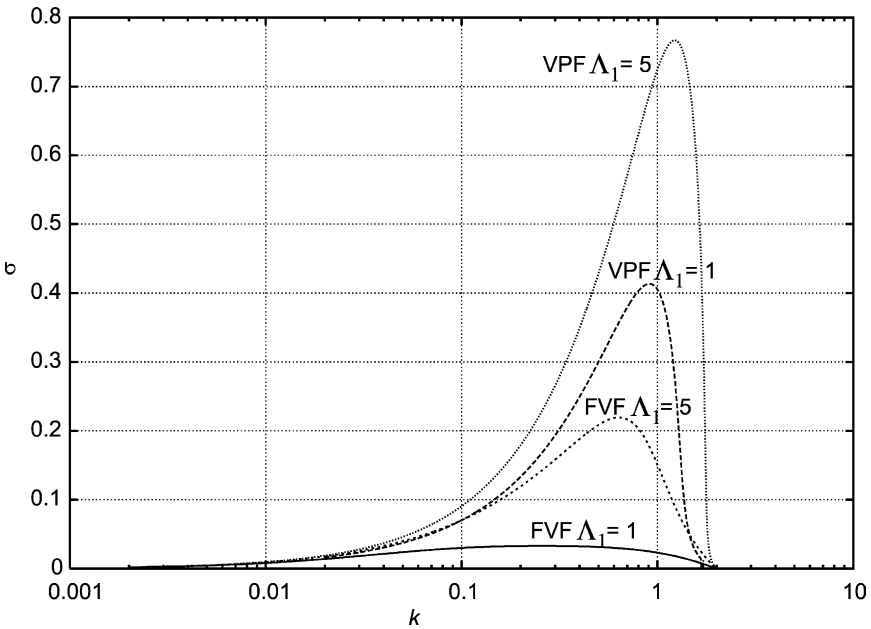

Fig. 8. PAA: $\Lambda_1 = 1, 5$.

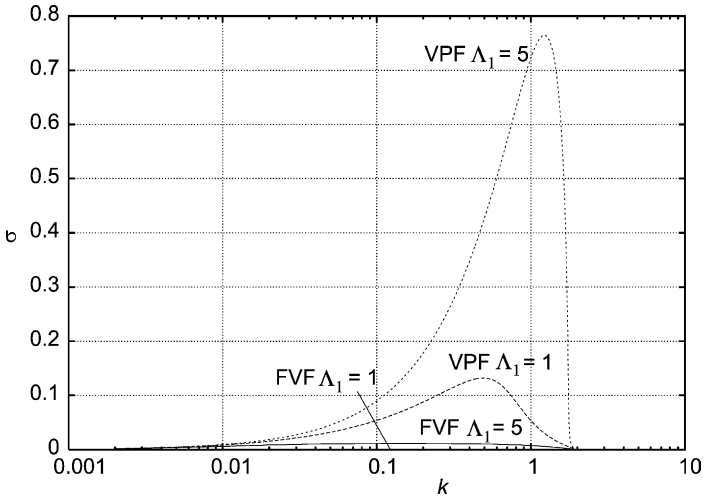

Fig. 9. PO: Λ_1 =1, 5.

Solving this, we have

$$\sigma = -\frac{1 - f\hat{\lambda}_1}{2\hat{\lambda}_2} \pm \sqrt{\left(\frac{1 - f\hat{\lambda}_1}{2\hat{\lambda}_2}\right)^2 + \frac{f}{\hat{\lambda}_2}}, \tag{45}$$

when $\hat{\lambda}_2 \neq 0$. The solution with the upper sign becomes $\sigma = f(k)$ if $\hat{\lambda}_2 = \hat{\lambda}_1$ (viscous fluid). For k small, $f(k) \approx \sqrt{J}/3(1 - (kR)^2)$, which corresponds to Rayleigh's case [3].

When $\hat{\lambda}_2 = 0$ in (44), we have $\sigma = f(k)/(1 - \hat{\lambda}_1 f(k))$, which is larger than $f(k)$ if $(1 - \hat{\lambda}_1 f(k)) > 0$; this growth rate has the larger value than that of the inviscid potential flow.

For the viscoelastic potential flow, (38) reduces to

$$\begin{vmatrix} I_1(kR) & K_1(kR) \\ G_1 & G_3 \end{vmatrix} = 0, \tag{46}$$

which is arranged as the quadratic equation of σ:

$$2\frac{k^2}{\sqrt{J}}(B + B_1\sigma)\sigma + C(1 + \hat{\lambda}_1\sigma) = 0. \tag{47}$$

For the single column given by $m = 0$ and $\hat{\lambda}_2 = 0$, (47) reduces to linear equation to give the solution σ:

$$\sigma = -\left[\frac{2k^2\beta}{C\sqrt{J}} + \hat{\lambda}_1\right]^{-1}. \tag{48}$$

When $\hat{\lambda}_1 = 0$, we have $\sigma = \sqrt{J}$ at $k = 0$ (the maximum growth rate in the limit $J \to 0$ for the viscous potential flow [13]).

5. Results

The data on viscoelastic fluids is provided for the diameter of the column $D = 1$ cm in Table 1. The peak values and the associated wavenumber are listed in Table 2, from the growth rate curves in Fig. 2 for PAA and Fig. 3 for PO. The growth rate and the wavenumber are shown in Figs. 4–7 for various values of Λ_1. The comparison of VPF and FVF are shown in Figs. 8 and 9. The growth rates in both theories increase with Deborah number at each fixed Reynolds number.

The growth rate and the wavenumber are shown in Figs. 10 and 11 for changing $\sqrt{J}$, and all theories collapse to inviscid potential flow for any fixed Deborah number as the Reynolds number tends to infinity.

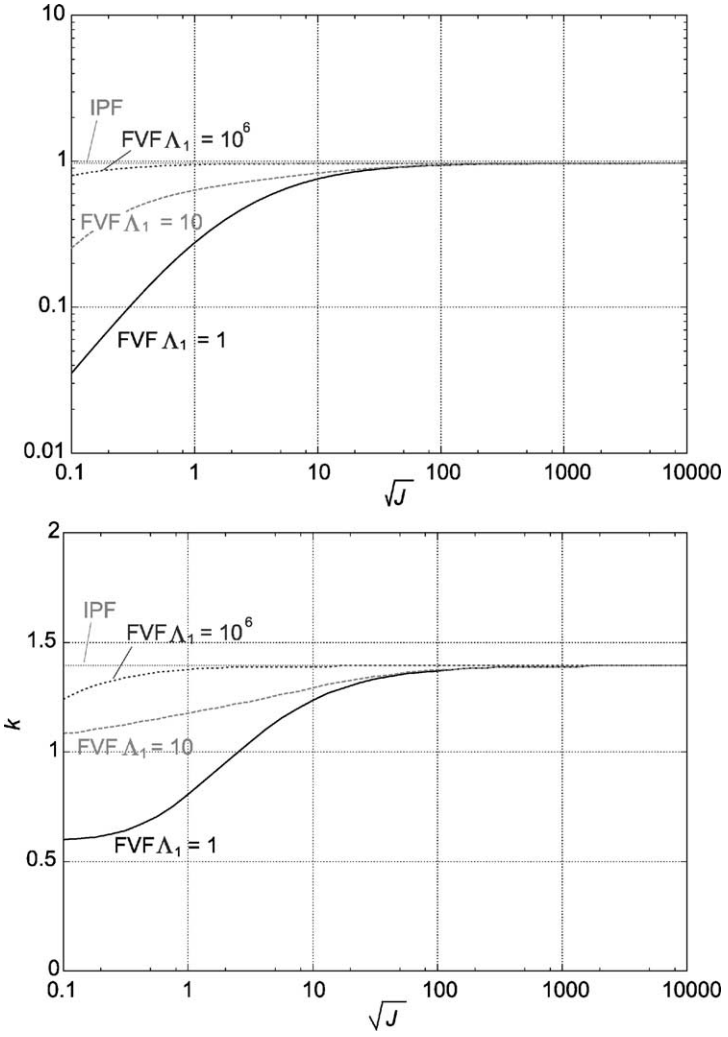

Fig. 10. The σ_m and k_m vs. $\sqrt{J}$ for FVF for $\Lambda_1 = 1.0, 10, 10^6$. The maximum growth rate of IPF is given by $\sigma_m = 0.97099$ at $k_m = 1.3957$, which is drawn for reference in the figure.

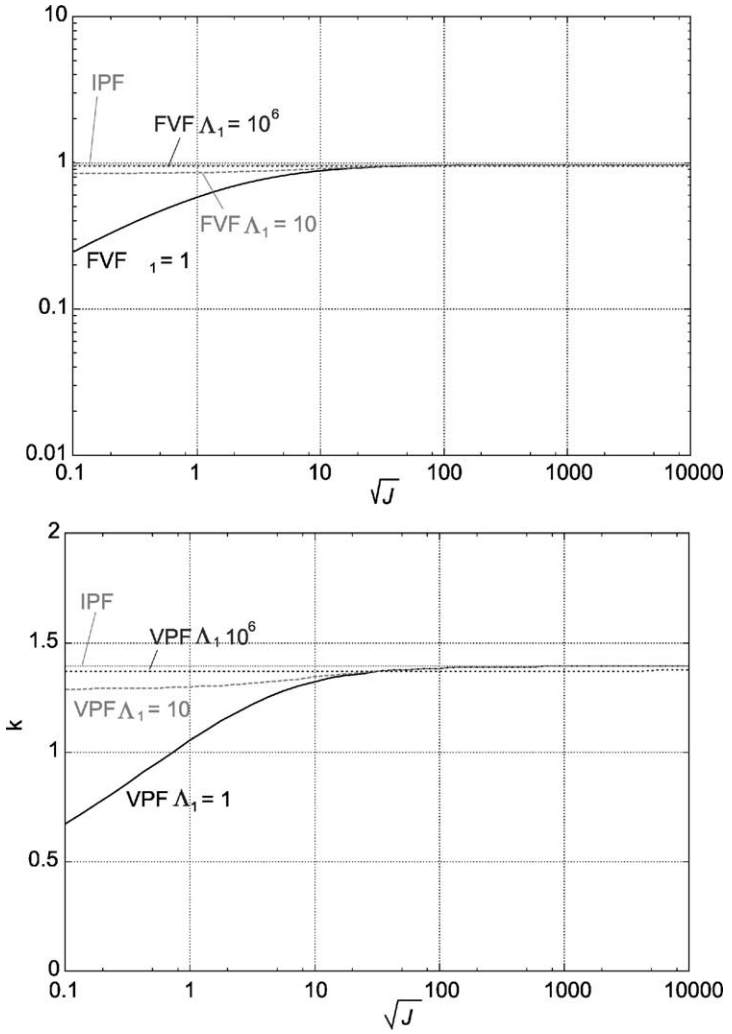

Fig. 11. The σ_m and k_m vs. $\sqrt{J}$ for VPF for $\Lambda_1 = 1.0, 10, 10^6$. The maximum growth rate of IPF is given by $\sigma_m = 0.97099$ at $k_m = 1.3957$, which is drawn for reference in the figure.

6. Conclusions and discussion

The following conclusions arise from our study of the linearized theory of capillary instability of a viscoelastic filament of Maxwell type in air. For many viscoelastic fluids the final stage of collapse is controlled by nonlinear effects not considered here.

- Capillary collapse is controlled by two parameters, a Reynolds number $J = \gamma D\rho/\mu^2$ and a Deborah number $\Lambda_1 = \gamma\lambda_1/\mu D$. The density ratio $\ell = \rho_a/\rho$ and viscosity ratio $m = \mu_a/\mu$ are small and have only a small effect.

- The dispersion relation for viscoelastic potential flow can be solved for σ and computed for any value of Λ_1.
- The dispersion relation for fully viscoelastic flow (where the shear stress and tangential velocity conditions are enforced) must be solved by iteration which breaks down at high Λ_1.
- Following earlier studies, we found that a disturbance will grow more rapidly on a viscoelastic filament than on a Newtonian liquid; the growth rates increase with Λ_1 at a fixed J.
- The growth rates for viscoelastic potential flow are several times larger than for fully viscoelastic flow for each fixed J when J is not large. The dispersion relation σ versus k and the peak value k_{m} and $\sigma_{\mathrm{m}} = \sigma(k_{\mathrm{m}})$ are not greatly different.
- As in our study [13] of capillary instability of viscous threads, all theories collapse to the inviscid theory in the limit of large J even when Λ_1 is huge. Inertia beats viscoelasticity when $J \to \infty$. The ratio $\Lambda_1/J = \lambda_1\mu/\rho D^2 = E$ is the elasticity number. Figs. 10 and 11 show that inertia beats elasticity even when E is rather large.
- The effect of increasing the retardation time Λ_2 ($0 \leq \Lambda_2 \leq \Lambda_1$) is to drive growth to Newtonian values.

Nonlinear studies of capillary instability are frequently framed in terms of extensional flow. Such studies are particularly popular in the rheology community. Purely extensional flow can be obtained from a potential; it is a potential flow. Potential flows must be irrotational, but strong effects of viscosity and viscoelasticity can be represented. Evaluation of the utility of potential flow solutions requires comparison with exact results. Here and in the other studies of stability reviewed in Section 1 we find very accurate results from viscous and viscoelastic potential flow when the appropriate Reynolds number is not too large. Even at low J, say those for Figs. 2 and 3 the discrepancy in the peak values is not greater than about two and the wave numbers for maximum growth are not greatly different. In general, the peak values are much closer even for Reynolds numbers in which inviscid potential flow is way off the mark. In the present case, and in many other cases, the potential flow solution can be done analytically, here even in cases in which the numerical simulations giving the exact results fail.

The main advantage of the viscous and viscoelastic potential studies is the determination of the conditions under which the flows are very nearly potential flows. This means that *vorticity*, not *viscosity* is negligible. For example, we could think of ways to connect the vorticity boundary layers on a flat plate to the potential flow of say glycerin in the free stream. We simplify the analysis using potential flow.

The observed dynamics of collapsing Newtonian and viscoelastic filaments is determined by nonlinear effects not considered in our linear analysis. Focusing now on the dynamics of thread rupture, in the Newtonian case, we consider the possibility that the main events prior to rupture are governed by viscous potential flow. The final event is universally, described as a pinch-off and the fundamental physics governing the rupture of the thread is not considered. A pinch-off is a squeezing flow; the radius of the jet at the pinch point collapses, squeezing fluid out as the filament collapses. Here one finds a stagnation point; stagnation point flow is a potential flow and the effects of viscosity in such a flow may be huge, even more so in the viscoelastic case where extensional flow = stagnation point flow is so important. Certainly, potential flow of an inviscid fluid is not the right tool here. We can get results in which viscosity acts strongly using viscous potential flow. The question is not whether viscosity is important, which it is, but whether vorticity is important.

Chen et al. [20] have studied pinch-off and scaling during drop formation using high-accuracy computation and ultra-fast high-resolution imaging. They discuss dynamic transition from potential flow with a 2/3 scaling due to Keller and Miksis [21] to an inertial-viscous regime described by Eggers' [22] universal

solution. They find overturn before breakup in experiments in water (1 cp) well before the dynamic transition from the potential flow to the inertial-viscous regime. On the other hand, an 85 cp glycerol–water solution is said to exhibit this transition. The potential flow solutions discussed by Chen et al. [20] are for inviscid solutions. Of course, water and glycerol are not inviscid. The scaling of Keller and Miksis [21] which gives rise to the 2/3 power collapse law does not work for viscous potential flow. The spoiler is their equation (3.3) expressing the normal stress balance. To this equation we must add the viscous component $2\mu\partial U_n/\partial n$. The term $(\nabla\phi)^2$ in (3.3) scales like ϕ^2/L^2 whereas the viscous component scales like ϕ/L^2, so that the similarity transformation does not factor through. Analogies have been put forward between capillary pinch-off of a viscous fluid thread and van der Waals driven ruptures of a free thin viscous sheet [23]. The observation that a filament under capillary collapse ruptures in a "pinch-off" does not come to grips with the physics which leads to a loss of the continuum. One idea is that thread breaks under the action of disjoining pressures. Unfortunately, a mathematical theory for disjoining pressures for thin threads is not available.

Another idea is that the high extensional stresses which are generated in the pinch region at rupture are the cause of the rupture, the rupture may be framed as a stress induced cavitation following ideas introduced by Joseph [24,25]. Cavitation will occur in pure extension when the extensional stress is large enough, at high rates of extension.

The idea that threads will break under tension at high rates of extension is particularly interesting for viscoelastic fluids which can support large extensional stresses. Small bubbles of vapor and gas could be expected to appear in the solvent of polymeric liquids or polymer melts when the thread enters into tension. The breaking of polymer strands on a spinline observed by Wagner et al. [26] was framed in terms of this maximum tension leading to cavitation by Joseph [25]. Wagner et al. claim that the breaking stress is a pure material constant which in their LDPE and HDPE samples is about 10^6 Pa, an order of magnitude larger than atmospheric; the thread is in tension when it breaks.

Lundgren and Joseph [27] analyzed the breakup of a capillary filament assuming extensional flow at the pinch point $(z = r = 0)$, $u_z = a(\mu, \gamma, t)z$, $u_r = -(1/2)a(\mu, \gamma, t)r$ where γ is surface tension and μ is viscosity. This is a viscous potential flow with a potential

$$\phi = \tfrac{1}{2}az^2 - \tfrac{1}{4}ar^2. \tag{49}$$

They found that the principal balance is between surface tension producing the neckdown and the viscosity which resists collapse; that the neck is of parabolic shape and its radius collapses to zero in a finite time. During the collapse the tensile stress due to viscosity increases in value until at a certain finite radius, which is about 1 μm for water in air, the stress in the throat passes into tension, presumably inducing cavitation there. The Reynolds number $Re = R_c\gamma\rho/\nu^2$ based on the velocity λ/μ of capillary collapse where $R_c = 1\,\mu$m is about 55. The solution of Lundgren and Joseph is flawed, it satisfies normal stress balance only at $z = 0$ but not elsewhere. However, it should be possible to compute an exact numerical solution of capillary collapse based on the equations of viscous potential flow in much the same way that capillary breakup was studied by numerical simulation of the equations for potential flow of an inviscid fluid by Mansour and Lundgren [28].

The recent literature on capillary collapse is presently dominated by the discovery of self-similar, finite time singularity formation. These solutions are discussed in the recent papers Chang et al. [16], McKinley and Tripathi [29], and in the paper of Chen et al. [20]. This literature does not treat the physics of rupture or breakup by cavitation and does not compute stresses. All of the above mentioned authors find that capillary radius decreases to zero linearly in time, but the rate of collapse differs from author to author.

McKinley and Tripathi [29] write the formula

$$R_{\text{mid}}^{(t)} = R_1 - \frac{2X-1}{6}\frac{\gamma}{\mu}t, \tag{50}$$

for the neck radius of the collapsing capillary in the stage of final decay as t increases to t^* when $R_{\text{mid}}^{(t^*)} = 0$. They give the X obtained by different authors in their Table 1, but without the value $X = 2$ obtained by Lundgren and Joseph [27] for viscous potential flow, who give the fastest decay. Eggers [7,22] obtained $X = 0.5912$ and Papageoriou [30] obtained $X = 0.7127$. The solutions of the two authors last named have vorticity; Papageriou's solution has no inertia. McKinley and Tripathi [29] note that very close to breakup the solution of Papageriou crosses over to Egger's similarity solution. Maybe the final breakup is a non-similarity solution which crosses over from Egger's solution to rupture.

The solution of Eggers [22] gives rise to a universal scaling law which has been observed for viscous liquids but not in water (see [20]). The long wave approximation used to derive universal scalings may prevent it from resolving the dynamics of rupture. The similarity solution of Eggers does not lead to a cavitation threshold; in his solution the tension due to extension increases but not fast enough to overcome the compression due to the capillary pressure of the thinning filament.

The criterion for the termination of the continuum is probably not a finite time singularity; the thread radius does not go to zero. It comes apart before then. The physics of rupture is up for discussion.

Acknowledgements

This work was supported by the NSF/CTS-0076648, the Engineering Research Program of the Office of Basic Energy Sciences at the DOE and by an ARO grant DA/DAAH04.

References

[1] L. Rayleigh, On the capillary phenomena of jets, Proc. Roy. Soc. London A 29 (1879) 71–79.
[2] Plateau, Statique experimentale et theorique des liquide soumis aux seules forces moleculaire, vol. ii, 1873, p. 231.
[3] L. Rayleigh, On the instability of a cylinder of viscous liquid under capillary force, Phil. Mag. 34 (207) (1892) 145–154.
[4] C. Weber, Zum Zerfall eines Flüssigkeitsstrahles. Ztschr. f. angew, Math. Mech. 11 (2) (1931) 136–154.
[5] S. Tomotika, On the instability of a cylindrical thread of a viscous liquid surrounded by another viscous fluid, Proc. Roy. Soc. London A 150 (1935) 322–337.
[6] S. Chandrasekhar, Hydrodynamic and Hydromagnetic Stability, Oxford University Press, Oxford, 1961.
[7] J. Eggers, Nonlinear dynamics and breakup of free-surface flows, Rev. Mod. Phys. 69 (3) (1997) 865–929.
[8] W.K. Lee, R.W. Flumerfelt, Instability of stationary and uniformly moving cylindrical fluid bodies. I. Newtonian systems, Int. J. Multiphase Flow 7 (2) (1981) 363–383.
[9] D.D. Joseph, T.Y. Liao, Potential flows of viscous and viscoelastic fluids, J. Fluid Mech. 265 (1994) 1–23.
[10] D.D. Joseph, J. Belanger, G.S. Beavers, Breakup of a liquid drop suddenly exposed to a high-speed airstream, Int. J. Multiphase Flow 25 (1999) 1263–1303.
[11] D.D. Joseph, G.S. Beavers, T. Funada, Rayleigh–Taylor instability of viscoelastic drops at high Weber numbers, J. Fluid Mech. 453 (2002) 109–132.
[12] T. Funada, D.D. Joseph, Viscous potential flow analysis of Kelvin–Helmholtz instability in a channel, J. Fluid Mech. 445 (2001) 263–283.
[13] T. Funada, D.D. Joseph, Viscous potential flow analysis of capillary instability, Int. J. Multiphase Flow 28 (9) (2002) 1459–1478.

[14] S. Middleman, Stability of a viscoelastic jet, Chem. Eng. Sci. 20 (1965) 1037.
[15] M. Goldin, J. Yerushalmi, R. Pfeffer, R. Shinnar, Breakup of laminar capillary jet of a viscoelastic fluid, J. Fluid Mech. 38 (1969) 689–711.
[16] H.-C. Chang, E.A. Demekhin, E. Kalaidin, Interated stretching of viscoelastic jets, Phys. Fluids 11 (7) (1999) 1717–1737.
[17] D.W. Bousfield, R. Keunings, G. Marrucci, M.M. Denn, Nonlinear analysis of the surface tension driven breakup of viscoelastic filaments, J. Non-Newtonian Fluid Mech. 21 (1986) 79–97.
[18] V.M. Entov, J. Eng. Phys. 34 (1978) 159–164.
[19] D.D. Joseph, Fluid Dynamics of Viscoelastic Flows, Springer, Berlin, 1990.
[20] A.U. Chen, P.K. Notz, O.A. Basaran, Computational and experimental analysis of pinch-off and scaling, Phys. Rev. Lett. 88 (17) (2002) 1745011–1745014.
[21] J.B. Keller, M.J. Miksis, Surface tension driven flows, SIAM J. Appl. Math. 43 (2) (1983) 268–277.
[22] J. Eggers, Universal pinching of 3D axisymmetric free-surface flow, Phys. Rev. Lett. 71 (1993) 3458.
[23] D. Vaynblat, J.R. Lister, T.P. Witelski, Symmetry and self-similarity in rupture and pinchoff: a geometric bifurcation, Eur. J. Appl. Math. 12 (3) (2001) 209–232.
[24] D.D. Joseph, Cavitation in a flowing liquid, Phys. Rev. E 51 (3) (1995) R1649–R1650.
[25] D.D. Joseph, Cavitation and the state of stress in a flowing liquid, J. Fluid Mech. 366 (1998) 367–378.
[26] M.H. Wagner, V. Schulze, A. Göttfert, Rheotens-mastercurves and drawability of polymer melts, Polym. Eng. Sci. 36 (7) (1996) 925–935.
[27] T.S. Lundgren, D.D. Joseph, Capillary Collapse and Rupture, unpublished paper, 1997 (http://www.aem.umn.edu/people/faculty/joseph/archive/docs/capillary.pdf).
[28] N.N. Mansour, T.S. Lundgren, Satellite formation in capillary jet breakup, Phys. Fluids A 2 (1990) 114.
[29] G.H. McKinley, A. Tripathi, How to extract the Newtonian viscosity from capillary breakup measurements in a filament rheometer, J. Rheol. 44 (3) (2000) 653–671.
[30] D.T. Papageriou, On the breakup of viscous liquid threads, Phys. Fluids 7 (1995) 1529.